

Revealing New Possibilities of Ultrashort Pulse Decomposition in a Turn of Asymmetrical Meander Delay Line

Alexander V. Nosov, Roman S. Surovtsev

Tomsk State University of Control Systems and Radioelectronics, Tomsk, Russia

Abstract – The paper describes the study of the turn of meander delay line (ML) with broad-side coupling protecting against ultrashort pulse. The work presents the results of a detailed analysis of the ultrashort pulse decomposition and reveals the appearance of an additional pulse between the mode pulses which arises due to the asymmetry of the cross section of the structure. The attenuation of the ultrashort pulse amplitude up to 3 times is achieved.

Index Terms – Ultrashort pulse, modal filtering, even mode, odd mode, protection, meander delay line.

I. INTRODUCTION

THE USE OF RADIOELECTRONIC EQUIPMENT (REE) in various spheres of social activity has made each person of this society dependent on the REE uninterrupted operation. Development trends of modern REE require the increase of performance and miniaturization of target devices, which leads to reduction of operation voltage levels. Due to low operating voltages, the sensitivity of REE to various electromagnetic interferences (EMI) increases, which can be the result of both natural (secondary lightning effects) or intentional (electromagnetic weapons) actions. Danger is caused by possibility of using EMI generators by criminal people aimed at destroying or disrupting REE of the critical objects of social infrastructure (electromagnetic terrorism), e.g. objects of fuel and energy complex [1]. The importance of this issue is proved by a number of cases of such effect, registered in different countries of the world [2].

II. PROBLEM STATEMENT

Protection of REE against ultrashort pulses which have short duration and high amplitude is currently of vital importance. As a result of experimental studies, it was shown that the measure of the induced energy is determined not by the total duration of an ultrashort pulse, but by its energy in a specific frequency range which is critical for this equipment [3]. However, the ultrashort pulse, even with a relatively low energy, can be destructive to sensitive REE. Traditional devices often cannot provide consistent protection for REE against ultrashort pulses due

to their drawbacks, such as low power or performance [4], e.g. operating time of a protective varistor can reach 25 ns. In addition, traditional protection devices have a limited operation life. Moreover, because of semiconductor components in their structure, they are heavily affected by radiation. This is unacceptable for space industry due to the tendency to increase the active life of a spacecraft up to 15 years. Finally, the efficiency of filters with lumped elements can be reduced as a result of the parasitic capacitance of the inductor at high frequencies and the possibility that an ultra-wideband signal enters the device through this capacitance [5]. Capacitors are susceptible to electrical breakdown: under the influence of a strong electric field, the dielectric between the plates loses insulating properties and begins conducting electric current [6]. Therefore, the search for new alternative protection devices is relevant.

Thus, devices for protecting equipment against ultrashort pulses, which are based on printed structures and signal filtering in the frequency band, are widely studied [7–12]. A noteworthy approach is the one in [13], which for the first time proposed and demonstrated in practice the technology/technique for decomposing an ultrashort pulse in meander delay lines (ML) into a sequence of pulses of lower amplitude. It is proved that the ultrashort pulse can be decomposed into a sequence of three main pulses with attenuation up to 6.3 times in an ML based on a microstrip line and up to 4.6 times in an ML with broad-side coupling. This approach is devoid of specifying drawbacks. Its use in REE may not require any protection device, since its implementation can rely on the interconnections which already exist on the PCB.

Another similar approach is the use of modal distortion to decompose ultrashort pulses in multiconductor printed devices: modal filters [14]. The authors in [15] have revealed the possibility that ultrashort pulses decompose in asymmetrical modal filters with additional pulses appeared during decomposition, due to which it is possible to increase the attenuation of an ultrashort pulse. Note that the ML structure with broad-side coupling from [13] is asymmetrical; however, the analysis of the possibility of ultrashort pulse decomposition in such structure has been performed without considering additional pulses.

The aim of this paper is to perform the study of a meander line with broad-side coupling, which takes into

account additional pulses, and to evaluate the possibility to additionally minimize the output signal. To achieve this aim, it is necessary to perform an analysis of asymmetric meander delay line with broad-side coupling, which has different parameters of its cross-section; to show the appearance of an additional pulse and to determine its characteristics; to formulate the condition of ultrashort pulse decomposition which takes into account the additional pulse; to present new simulation results and to analyze them.

III. RESULTS

The simulation was performed using the TALGAT system [16], which implements the calculation of transmission line parameter matrices with the method of moments and the time response with the node-potential method [17]. Also, we note that the method of moments is widely used and proved itself to be good for simulating meander delay lines [18–19].

A. Revealing an additional pulse

First, let us consider the paper [20], which shows the decomposition of an ultrashort pulse in an ML with broad-side coupling and the minimization of the ultrashort pulse. Fig. 1a shows the cross-section with parameters from [20] where: the width and thickness of the signal conductor $w=15 \mu\text{m}$ and $t=105 \mu\text{m}$ respectively; the separation between the conductors $s=1 \text{mm}$, the PCB substrate thickness $h=6 \text{mm}$; the distance from the structure edge to the signal conductor $d=3w$; the dielectric permittivity of the substrate $\epsilon_r=4$. Fig. 1b shows the circuit diagram of the turn.

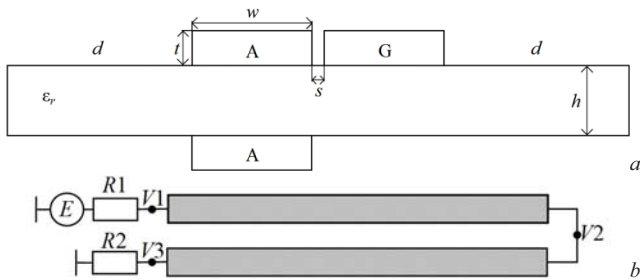


Fig. 1. Cross-section (a) and circuit diagram (b) of ML with broad-side coupling.

The line consists of two parallel conductors, each with the length of $l=1 \text{m}$, interconnected at the far end. One of the conductors is connected to a pulse source in the near end, which is presented by the electromotive force source E and the internal resistance $R1$. Another conductor of the line is connected to a receiving unit, which is presented in the diagram as resistance $R2$. To minimize reflections, resistances $R1$ and $R2$ are taken equal to the geometric mean of the characteristic impedance of even and odd modes (including further simulation, when the structure parameters are changed).

Calculated matrices of per-unit-length coefficients of electrostatic (\mathbf{C}) and electromagnetic (\mathbf{L}) inductances of the structure from Fig. 1a are the following:

$$\mathbf{C} = \begin{bmatrix} 137.89 & -96.94 \\ -96.94 & 122.44 \end{bmatrix} \text{ pF/m,}$$

$$\mathbf{L} = \begin{bmatrix} 382.92 & 269.55 \\ 269.55 & 477.22 \end{bmatrix} \text{ nH/m.}$$

Then, we calculated the response to the ultrashort pulse with e.m.f. amplitude of 1 V and durations of rise time, flat top and fall time of 1 ns. Fig. 2 shows the voltage waveform at the end of the turn.

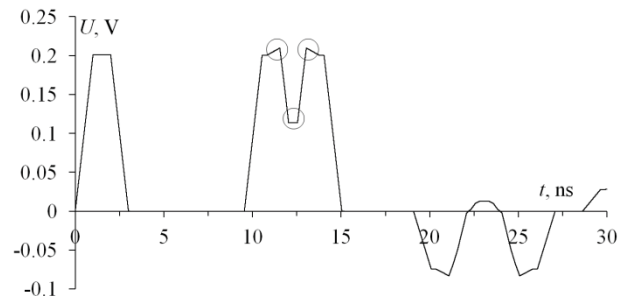


Fig. 2. Voltage waveform at the end of ML with broad-side coupling.

As it can be seen from the voltage waveform, the ultrashort pulse at the end of the ML with broad-side coupling became a sequence of three main pulses of smaller amplitude, not exceeding 0.210 V. The first pulse is near-end crosstalk, the second and third ones are pulses of the even and odd modes of the line. However, there is a step with amplitude of 0.114 V between the pulses of the even and odd modes of the line. There are also signal bursts on the fall and the front of the second and third pulses, respectively.

In another paper [13], the effect of changing the parameters of an ML with broad-side coupling on the ultrashort pulse attenuation has been examined in detail. The optimal meander line parameters ensuring the fulfillment of the conditions were obtained

$$2\tau_e l \geq t_\Sigma, \quad (1)$$

$$2l|\tau_e - \tau_o| \geq t_\Sigma \quad (2)$$

where τ_e and τ_o are per-unit-length delays of even and odd line modes, respectively, and t_Σ is the total ultrashort pulse duration.

The fulfillment of condition (1) provides the arrival of the even mode pulse after the end of the crosstalk pulse, and (2) – the decomposition of the main pulse into even and odd mode pulses. Also, the optimization of the coupling between the signal conductors allows equalizing the amplitudes of these three pulses, and therefore, minimizing the amplitude of the output signal. The optimal parameters of the ML with broad-side coupling from [13] are the following: $w=1000 \mu\text{m}$, $t=18 \mu\text{m}$, $s=200 \mu\text{m}$, $h=540 \mu\text{m}$, $d=3000 \mu\text{m}$, $\epsilon_r=5$, $l=80 \text{mm}$.

Calculated \mathbf{C} and \mathbf{L} matrices are:

$$\mathbf{C} = \begin{bmatrix} 128.89 & -93.5116 \\ -93.5116 & 120.31 \end{bmatrix} \text{ pF/m,}$$

$$\mathbf{L} = \begin{bmatrix} 487.441 & 332.564 \\ 332.564 & 572.637 \end{bmatrix} \text{ nH/m.}$$

Per-unit-length delays of even and odd modes of the investigated structure were calculated: $\tau_e=5.14$ ns/m, $\tau_o=6.56$ ns/m. The waveform of the output signal (Fig. 3) in the line corresponding to the selected parameters is considered in detail. An ultrashort pulse with e.m.f. amplitude of 1 V and durations of flat top of 100 ps, rise time and fall time of 50 ps, taken the same as in [13].

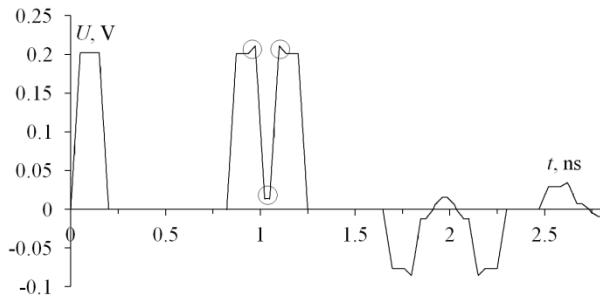


Fig. 3. Voltage waveform at the end of ML with broad-side coupling for $l=80$ mm.

As it can be seen from the signal waveform, the ultrashort pulse at the end of the line is decomposed into three main pulses. In this case, the maximum signal amplitude at the end of the line does not exceed 0.202 V. It is important to note that between the even and odd mode pulses of the line we observed a step, similar to the one in Fig. 2, but with smaller amplitude, not exceeding 12 mV; and signal bursts are still observed at the fall and front of the second and third pulses. For clear demonstration of the presence of the pulse between the even and odd modes, we calculated the response when the line length increases. Fig. 4 shows the calculated voltage waveform at $l=150$ mm.

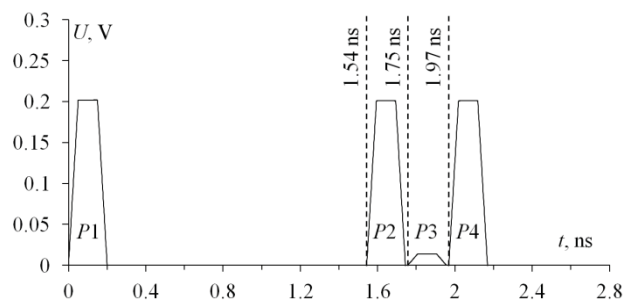


Fig. 4. Voltage waveform at the end of ML with broad-side coupling for $l=150$ mm.

It is seen that the ultrashort pulse is presented by a sequence of 4 pulses: crosstalk ($P1$), even mode ($P2$), additional ($P3$), and odd mode ($P4$). We define the delays of each of them. Since pulse $P1$ is a crosstalk, its arrival time is $t_1=0$ ns. The delay of pulse $P2$ (even mode pulse) is defined as $t_2=\tau_e 2l=1.54$ ns and the delay of pulse $P4$ (odd mode pulse) is $t_4=\tau_o 2l=1.97$ ns. The delay of the additional

pulse ($P3$) is defined as the arithmetic mean of the delays of the even and odd mode pulses, and amounts $t_3=(\tau_e 2l+\tau_o 2l)/2=1.75$ ns. After determining the delays of each of the pulses, we can formulate the conditions for the complete decomposition of the ultrashort pulse into 4 pulses (crosstalk, even mode, additional pulse and odd mode). We note that the condition which provides the arrival of the even mode pulse after the end of the crosstalk pulse corresponds to condition (1). The second condition provides the arrival of the additional pulse at the end of the even mode pulse – $t_3 \geq t_2 + t_{\Sigma}$, and the third condition provides the arrival of the odd mode pulse at the end of the additional pulse – $t_4 \geq t_3 + t_{\Sigma}$. After the substitution of the known variables and algebraic transformations, the second and third conditions will take the same view

$$l(\tau_o - \tau_e) \geq t_{\Sigma}. \quad (3)$$

After substitution of the known values in (1) and (3), we obtain $1.54 \text{ ns} \geq 0.2 \text{ ns}$ and $0.21 \text{ ns} \geq 0.2 \text{ ns}$, respectively. Thus, Fig. 4 shows the case when conditions (1) and (3) are satisfied and the ultrashort pulse is decomposed into 4 pulses. For the case in Fig. 3, when we substitute the known values in (1) and (3), we obtain $0.82 \text{ ns} \leq 0.2 \text{ ns}$ and $0.11 \text{ ns} < 0.2 \text{ ns}$, respectively. Thus, conditions (1) and (3) are not satisfied, and the ultrashort pulse is decomposed only into 3 pulses.

The existence of the additional pulse gives an additional resource to ultrashort pulse amplitude attenuation. For this, it is necessary to equalize its amplitude with the amplitudes of other pulses, therewith to minimize the total amplitude at the end of the line. It seems possible to do this due to parametric optimization of the structure.

B. Minimization of the output voltage amplitude

Before the optimization, it is useful to analyze the effect of the cross-section parameters of the line on the amplitudes of each of the 4 pulses. The initial parameters are chosen so as to provide the fulfillment of conditions (1) and (3) and to exclude the superposition of pulses with a separate change of each parameter in a given range: $w=500$ μm , $t=200$ μm , $s=25$ μm , $h=750$ μm , $d=1500$ μm , $\epsilon_r=200$, $l=80$ mm. The range and step of the variable parameters are the following: 100, 200, ..., 1000 μm for w , t and h ; 5, 10, ..., 50 μm for s ; 25, 50, ..., 300 for ϵ_r . Fig. 5 shows the obtained dependences of the amplitudes of each of the 4 pulses on w , t , s , h and ϵ_r .

As can be seen from Fig. 5, the increase of parameters t and s leads to the same change of the amplitudes of all 4 pulses. When t increases, the amplitudes of all pulses monotonically decrease, and when s increases, they increase too. The increase of ϵ_r does not lead to a significant change in the amplitudes of the pulses. There is only a slight increase of the $P4$ pulse amplitude in the range of 25–200. From the t , s , and ϵ_r dependences it is clear that the amplitude of the output signal is determined by the pulse $P3$ amplitude.

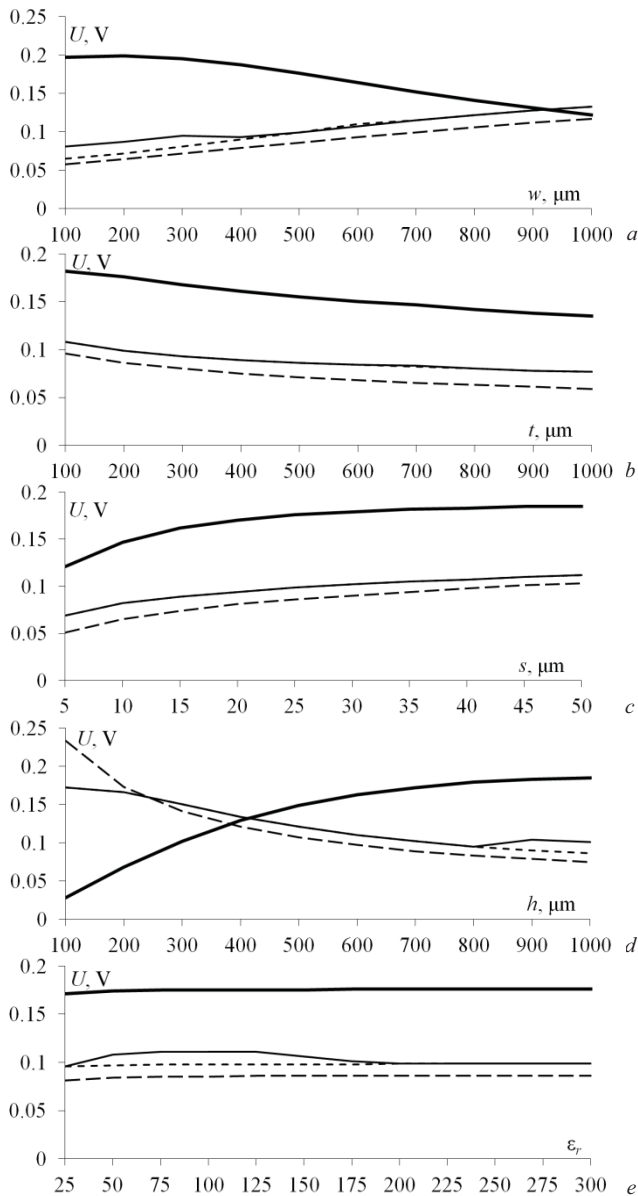


Fig. 5. Dependencies of $P1$ (---), $P2$ (-.-), $P3$ (—) и $P4$ (—) pulse amplitude at the end of asymmetrical ML from w (a), t (b), s (c), h (d) and ϵ_r (e) with the original unchanged parameters.

The dependences in Fig. 5a and Fig. 5d are interesting, since the increase of w leads to the increase of the $P1$, $P2$, and $P4$ pulse amplitudes and the decrease of the $P3$ pulse amplitude; and the increase of h leads to the increase of the $P3$ pulse amplitude and the decrease of the $P1$, $P2$, and $P4$ pulse amplitudes. It is also seen that there are values of w and h for which the amplitudes of all pulses are almost the same, only the $P1$ pulse has a slight difference in amplitude. Thus, the minimization of the amplitude at the end of the line is more possible by equalizing the amplitudes of $P2$ – $P4$ pulses. Based on this and taking into account conditions (1) and (3), using the heuristic search, we found the values of the optimal ML parameters from Fig. 1 according to the criterion of minimizing the amplitude of the output voltage: $w=380 \mu\text{m}$, $t=18 \mu\text{m}$,

$s=200 \mu\text{m}$, $h=940 \mu\text{m}$, $d=3w$, $\epsilon_r=20$, $l=150 \text{ mm}$. Fig. 6 shows the output voltage waveform for this values of parameters.

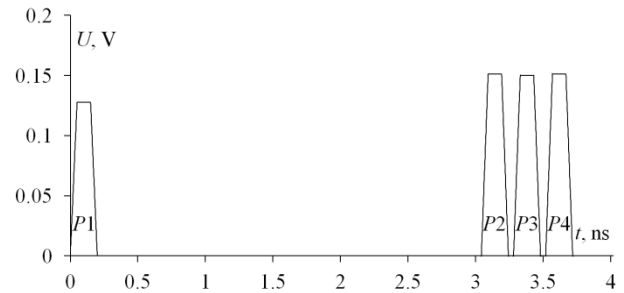


Fig. 6. Output voltage waveform for ML with optimal parameters.

It can be seen from the waveform that the $P2$, $P3$, and $P4$ pulse amplitudes have the same value of about 0.151 V, which determines the maximum amplitude at the end of the line. The amplitude of pulse $P1$ is 0.127 V. The maximum attenuation is about 3 times, against 2.3 times obtained in [13] and [20].

C. Additional results

A situation is possible when the pulses arrive at the end of the line with equal time intervals between pulses [13]. The condition for such arrival for three pulses is:

$$\tau_{max}=2\tau_{min}, \quad (4)$$

where τ_{min} and τ_{max} is the minimum and maximum of per-unit-length delays of the even and odd modes of the line, respectively. However, the condition (4) does not take into account the additional pulse; therefore, the time intervals between 4 pulses in Fig. 4 will not be equal. It is obvious, that, in order to take into account the additional pulse, condition (4) takes the form:

$$\tau_{max}=3\tau_{min}. \quad (5)$$

Consider the case when condition (5) is fulfilled. For this, we made an optimal parameter search; we obtained the following parameters: $w=1000 \mu\text{m}$, $t=136 \mu\text{m}$, $s=5 \mu\text{m}$, $h=1200 \mu\text{m}$, $d=3000 \mu\text{m}$, $\epsilon_r=500$, $l=80 \text{ mm}$. The calculated per-unit-length delays were $\tau_e=19.6 \text{ ns/m}$, $\tau_o=58.6 \text{ ns/m}$. Fig. 7 shows the voltage waveform under condition (5).

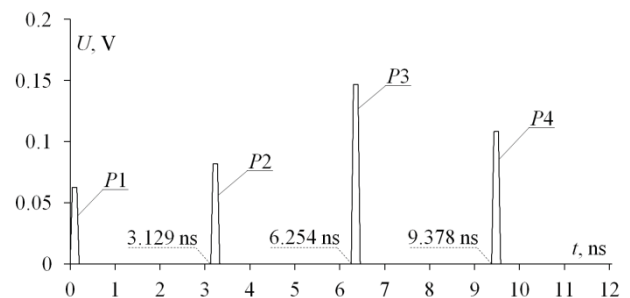


Fig. 7. Voltage waveform at the end of the ML under condition (5).

Fig. 7 shows that the ultrashort pulse at the end of the line became a sequence of pulses with equal time intervals between the pulses. After the arrival of the first 4 pulses, the pulses caused by reflections will arrive. The amplitude at the end of the line is 0.146 V.

IV. CONCLUSION

The work studied an ML with broad-side coupling which protects equipment against ultrashort pulse. The paper presents the results of the detailed analysis of ultrashort pulse decomposition of the turn of the ML with broad-side coupling, and reveals the existence of an additional pulse between the mode pulses of the line, which appears due to the asymmetry of the cross-section of the structure. It is demonstrated that the existence of an additional pulse is a resource for minimizing the output signal amplitude. The conditions providing the arrival of all decomposed pulses after the fall of the previous pulse are formulated. The cross-section parameters of the line are shown to have the influence on the amplitudes of the main decomposition pulses at the end of the line. It was revealed that the change of the signal conductor width and the dielectric substrate thickness has the greatest influence; and the signal amplitude minimum at the end of the line is determined by the additional pulse amplitude and the even and odd mode pulses of the line. The simulation example shown that due to the additional pulse, it is possible to increase the ultrashort pulse attenuation in the line. The maximum attenuation of ultrashort pulse amplitude up to 3 times is obtained. Finally, we formulated the condition which provides the arrival of each of 4 pulses to the line end with equal time intervals between the neighboring pulses.

ACKNOWLEDGMENT

The study was supported by the grant № 19-19-00424 of the Russian Science Foundation in TUSUR.

REFERENCES

- [1] E.N Fominich and D.R. Vladimirov "Elektromagnitnyj terrorizm. Novaya ugroza dlya informacionno-upravlyayushchih sistem [Electromagnetic terrorism. A new threat to management information systems]," *Voennyj inzhener*, vol. 2, no. 2, pp. 10-17, 2016 (in Russian).
- [2] O. Petkau et al., "Zashchita ob'ektov toplivno-energeticheskogo kompleksa ot ugroz elektromagnitnogo vozdeystviya [Protection of the fuel and energy complex against electromagnetic threats]," *Bezopasnost ob'ektov toplivno-energeticheskogo kompleksa*, vol. 2, no. 6, pp. 74-76, 2014 (in Russian).
- [3] C. Mojert et al., "UWB and EMP susceptiblity of microprocessors and networks," *Proc. of the 14th Int. Zurich Symp. on EMC*, Zurich, Switzerland, February 20–22, 2001, pp. 47–52.
- [4] Z.M. Gizatullin, R.M. Gizatullin, "Investigation of the immunity of computer equipment to the power-line electromagnetic interference," *Journal of Communications Technology and Electronics*, no. 5, 2016, pp. 546-550.
- [5] Zajkova S.A. "Passivnye komponenty radioelektronnoj apparatury [Passive components of electronic equipment]," *Posobie*, Grodno: GrGU, 2009, 67 p. (in Russian).
- [6] A.S. Koldunov, "Radiolyubitel'skaya azbuka. Analogovye ustrojstva [Radio alphabet. Analog devices]," *M: Solon-Press*, vol. 2, 2004, 288 p.
- [7] R. Krzikalla et al., "Systematic description of the protection capability of protection elements," in *Proc. of IEEE Int. Symp. on EMC*, Honolulu, HI, USA, 2007, pp. 1-4.

- [8] R. Krzikalla et al., "Interdigital microstrip filters as protection devices against ultrawideband pulses," in *Proc. of IEEE Int. Symp. on EMC*, Istanbul, Turkey, 2003, pp. 1313–1316.
- [9] R. Krzikalla and J.L. ter Haseborg, "SPICE simulations of UWB pulse stressed protection elements against transient interferences," in *Proc. of IEEE Int. Symp. on EMC*, Chicago, IL, USA, pp. 977–981, 2005.
- [10] T. Weber et al., "Linear and nonlinear filters suppressing UWB pulses," *IEEE Trans. on EMC*, vol. 36, no. 3, 2004, pp. 423–430.
- [11] Q. Cui et al., "Investigation of waffle structure SCR for electrostatic discharge (ESD) protection," in *IEEE International Conference on Electron Devices and Solid State Circuit (EDSSC)*, 2012, Bangkok, Thailand, Dec. 2012, pp. 3-5.
- [12] H. Hayashi et al., "ESD protection design optimization using a mixed-mode simulation and its impact on ESD protection design of power bus line resistance," in *International Conference on Simulation of Semiconductor Processes and Devices*, 2005 (SISPAD 2005), Tokyo, Japan, Sept. 2005, pp. 99-102.
- [13] A.V. Nosov, "Sovershenstvovanie zashchity radioelektronnoj apparatury ot sverhkorotkih impul'sov za schet meandrovyh linij zaderzki [Improving the protection of radio electronic equipment from ultrashort pulses using meander delay lines]," Ph.D. dissertation, Dept. Telev. and Cont., Tomsk State Univ. of Cont. Sys. and Radioelec., Tomsk, RF, 2018, 185 p. (in Russian).
- [14] A.O. Belousov et al., "Multicriteria optimization of multiconductor modal filters by genetic algorithms," in *2017 Siberian Symposium on Data Science and Engineering (SSDSE)*, Russian Federation, Novosibirsk, 2017 April 12-13, pp. 65-68.
- [15] A.T. Gazizov et al. "Time-domain response of asymmetrical modal filter without resistors to ultrashort pulse excitation," *17th International conference on micro/nanotechnologies and electron devices (EDM)*, June 30 – July 4, 2016, pp. 85–88.
- [16] S.P. Kuksenko et al., "Novyye vozmozhnosti sistemy modelirovaniya elektromagnitnoy sovmestimosti TALGAT," *Dokladi Tomsk. gos. un-ta sist. upr. i radioelektroniki*, vol. 2, no. 36, 2015, pp. 45-50. (in Russian)
- [17] J.R. Griffith and M.S. Nakhla, "Time-domain analysis of lossy coupled transmission lines," *IEEE Transactions on Microwave Theory and Techniques*, vol. 38, no. 10, pp. 1480–1487, 1990.
- [18] B.J. Rubin and B. Singh, "Study of meander line delay in circuit boards," *IEEE Trans. on Microwave Theory and Techniques*, vol. 48, pp. 1452–1460, 2000.
- [19] A.U. Bhoobe et al., "Meander delay line challenge problems: a comparison using FDTD, FEM and MoM," *Int. Symposium on EMC*, pp. 805–810, 2001.
- [20] A.T. Gazizov et al., "UWB pulse decomposition in simple printed structures," *IEEE Transactions on Electromagnetic Compatibility*, vol. 58, no. 4, Aug. 2016, pp. 1136–1142.



Alexander V. Nosov was born in Semipalatinsk, Kazakhstan in 1994. He received a Bachelor's degree, Master's degree and Ph.D. degree in radio engineering from Tomsk State University of Control Systems and Radioelectronics, Tomsk, Russia, in 2015, in 2017 and in 2018, accordingly. Currently, he is working as a Senior Researcher at TUSUR. He is the author and coauthor of 39 scientific papers.



Roman S. Surovtsev received an Engineering degree and the Ph.D. degree in radio engineering from Tomsk State University of Control Systems and Radioelectronics, Tomsk, Russia, in 2013 and 2016, accordingly. He is currently a Senior Researcher at TUSUR. He is the author and coauthor of 90 scientific papers, including one book.